Magnetic phase transitions of CeSb: Results of structure refinements

Fischer, P.; Hälg, W.; Muir, G.; Lebech, B.; Rainford, B.D.; Vogt, O.

Publication date:
1977

Document Version
Publisher's PDF, also known as Version of record

Risø Report No. 369

Magnetic Phase Transitions of CeSb: Results of Structure Refinements

by P. Fischer, G. Meier, W. Hälg, B. Lebech,
B. D. Rainford, and O. Vogt

September 1977

Sales distributors: Jul. Gjellerup, Sølvgade 87, DK-1307 Copenhagen K, Denmark
Available on exchange from: Risø Library, Risø National Laboratory, DK-4000 Roskilde, Denmark

UDC 546.655: 538.22: 548.78

September 1977 Risø Report No. 369

MAGNETIC PHASE TRANSITIONS OF CeSb: RESULTS OF STRUCTURE REFINEMENTS

by

P. Fischer[+], G. Meier[+], W. Hälg[+],
B. Lebech[*], B.D. Rainford[*†], and O. Vogt[§]

[+]Institut für Reaktortechnik ETHZ, c/o E.I.R.,
CH-5303 Würenlingen, Switzerland

[*]Physics Department, Risø National Laboratory,
DK-4000 Roskilde, Denmark

[§]Laboratorium für Festkörperphysik, ETH,
CH-8093 Zürich, Switzerland

[†]Permanent address: Physics Department, Imperial College,
London, U.K.

Risø Repro
ISBN 87-550-0503-9

ABSTRACT

The magnetic ordering of the anomalous antiferromagnet CeSb, which has a NaCl crystal structure, was determined in zero and non-zero applied magnetic fields by means of neutron diffraction investigations of single crystals and powder. Below the Néel temperature of (16.1±0.1) K, in zero field, there are six partially disordered magnetic phases of antiphase-domain type (<100> superstructures) with <100> orientation of the magnetic moments. At low temperatures and increasing magnetic fields, the structures transform from antiferromagnetic via ferrimagnetic configurations to a ferromagnetic state, i.e. the magnetic properties are similar to those of Ising spins. At higher temperatures (T>10 K) the existence of antiphase-domain-type superstructures along the tetragonal c axis implies considerable disorder even at high fields, and partially ordered, field-induced states exist even above the Néel temperature in zero field. Detailed results are given (structure factor tables) of the complete structure refinements at various temperatures for magnetic fields applied to the [001] direction.

CONTENTS

1. INTRODUCTION

The anomalous magnetic properties of CeSb (cf. the reviews published by Cooper (1976a,b)) are rather unique within the large class of rare-earth monopnictides that have a simple NaCl crystal structure, because of the interplay between the strongly anisotropic exchange interactions and the effects of the crystalline electric field, which are of a comparable order of magnitude. Also the associated magnetoelastic effects are of importance for the anomalous magnetic behaviour (Cooper 1976b). One anomaly in CeSb is the experimental fact that the easy axes of magnetization are along the <100> directions, while in sufficiently diluted $Ce_{1-x}(Y,La)_xSb$ the <111> directions are favoured as easy axes. In the diluted compounds, the anisotropic Ce-Ce interaction is decreased and therefore the easy direction is that characteristic of the crystal-field anisotropy alone (Cooper 1976a).

Recently, we summarized and discussed in detail the results obtained from an elastic neutron scattering investigation of single crystals and powder of CeSb in both zero (Fischer et al 1977) and non-zero (Meier et al 1978) applied magnetic fields. The present report is a compilation of the results of the structure refinements carried out in order to derive the phase diagram and determine the corresponding magnetic structures. In section 2 are listed the measured intensities and the structure factor tables. Section 3 gives the Fourier representation of the magnetic structures in both zero and non-zero applied magnetic fields.

2. RESULT OF STRUCTURE REFINEMENTS

2.1. Short Summary of the Experimental Procedures

Several CeSb single crystals and one powder sample were investigated in the present neutron diffraction study. The powdered sample was kindly supplied by Dr. N. Nereson from the University of Californis, Los Alamos, and was identical to that used by Nereson et al (1972). The single crystals were grown at the laboratory of solid state physics of the "Eidgenössische Technische Hochschule" in Zürich.

The investigations of the single crystals were carried out using neutrons of various incident wavelengths. The experimental details are summarized in table 1. Generally, the collimations in front of and behind the sample were defined by the dimensions of the monochromator, sample and detector. Whenever necessary

Table 1. Experimental details of the neutron diffraction studies.

Sample	No.	Dimensions (mm) x,y,z	Orientation (zone axis, ⊥)	Wave-length (Å)	Mono-chromator	Reactor
Single crystal	I	3,1,4	[001] / [0$\bar{1}$1]	1.71,1.76 / 1.17	Ge 111 / Be 002	DR 3/Riso
	II	3,2,2.5	[001]	1.71	Ge 111	DR 3/Riso
	III	3.7,3.1,4.8	[001]	1.03 / 1.05	C* 002	Saphir/Diorit/ Würenlingen
Powder V-container	IV	diameter 10 height 50		2.34	C* 002	Saphir/ Würenlingen

*pyrolytic graphite

+pyrolytic graphite and filter

the collimation in front of and after the sample was improved by Soller slits. Because of the limited resolution, the magnetic reflections are indexed in the pseudo-cubic cell.

The neutron diffraction measurements indicated that the magnetic structure of CeSb is sinusoidal. Such a structure gives rise to magnetic satellite peaks originating from the nuclear Bragg peaks. In the single crystals investigation these satellites were located in reciprocal space by performing systematic scans (general linear scans (Lebech and Nielsen 1975)) with equidistant steps in reciprocal space. These scans were preferentially parallel to symmetry directions, but other types of scans such as ω-scans (rock-scans) or θ-2θ scans through selected reciprocal lattice points were also used. In most cases θ-2θ scans were used to determine integrated intensities. For neutron wavelengths of the order of 1 Å, extinction, which presents no problem in powder measurements, appeared to be of minor importance. Only the most intense nuclear reflections were found to be affected by extinc-

tion and were therefore generally omitted from the refinements. Corrections for absorption are negligible and were not taken into account.

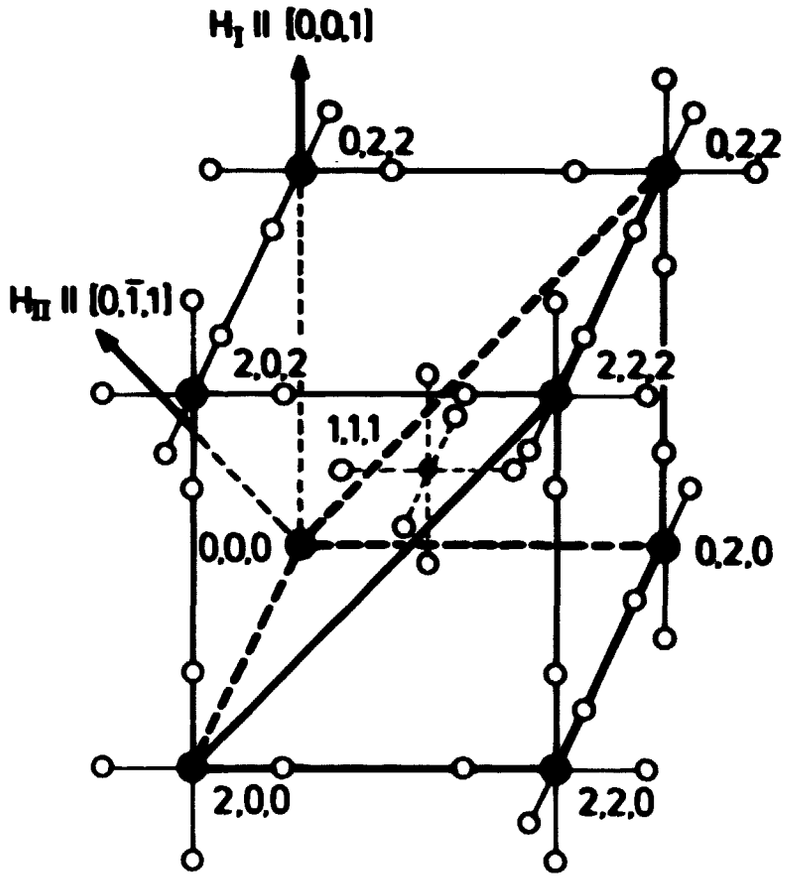

Figure 1. Section of the reciprocal space (pseudo-cubic) of CeSb showing the positions of magnetic satellite peaks (three domains along X, Y and Z) corresponding to a ++-- configuration (type IA). The filled circles indicate the nuclear Bragg reflections.

As illustrated in figure 1, the observed magnetic peaks may be indexed as magnetic satellites {±q00} of the nuclear Bragg reflections hkℓ, i.e. the magnetic peaks correspond to X, Y and Z domains of magnetic superstructures along the three <100> directions. The domain distribution is not a statistical one; generally, the Z domains were found to be favoured. Also shown in figure 1 are the directions ($\vec{H}_I$ and $\vec{H}_{II}$) of the applied magnetic fields. In the following we only consider the effects of applied fields parallel to the [001] direction ($\vec{H}_I$).

2.2. Structure Factor Tables

In the structure analysis we considered only commensurable magnetic superstructures. The results of the analysis are summarized in tables 2 and 3, which also list the number of Ce^{3+} layers (M) within a magnetic unit cell, the number of chemical cells (N) within a magnetic cell, and the position of the most

Table 2. Antiferromagnetic structures of CeSb in zero applied magnetic field. N is the number of chemical cells contained in the magnetic cell along [001] (c-domains), and M is the period of the magnetic structure, i.e. the number of Ce-layers. The magnetic structures are composed by the stacking of blocks of Ce^{3+} layers ($F_\pm$ and $D_\pm$) as described in section 2.2.

Phase	Temperature range (K)	Q	L_o/N	M	N	Ce^{3+} layer sequence in N chemical cells along [001]	Order (%)
I	15.9–16.1	0.666	2/3	3	3	$D_-D_+F_-$ (or + − 0 + −)	67
II	15.3–15.9	0.617	8/13	13	13	$F_+D_+D_-F_+D_+$ $F_+D_+D_-F_+D_-$	77
III	13.7–15.3	0.576	4/7	7	7	$F_+D_-F_-$ $F_+D_-F_-$	86
IV	11.0–13.7	0.555	5/9	9	10	$F_+D_-F_-F_-D_+F_-F_-$	89
V	8.9–11.0	0.545	6/11	11	11	$F_+F_-F_+D_-F_-$ $F_+F_-F_+D_-F_-$	91
VI	≤ 2.2– 8.9	0.506 ±0.002	1/2	2	4	F_+F_- (or + − − −)	100

intense magnetic satellite $Q = L_o/N$. The structures listed in table 2 (zero field) are composed of four simple, stacked blocks ($F_\pm$ and $D_\pm$). These blocks are combinations of layers of Ce atoms in which the Ce^{3+} moments are either completely disordered (paramagnetic layers) or completely ordered (ferromagnetically aligned parallel to [001]). The F_+ block consists of two ferromagnetic Ce^{3+} layers that are ferromagnetically coupled to each other. The D_+ block consists of a paramagnetic Ce^{3+} layer sandwiched between two ferromagnetic Ce^{3+} layers that are antiferromagnetically coupled to each other. In the notation used to describe the f.c.c. type IA antiferromagnetic structure (++−−), F_+ is described by ++ and D_+ by +0−. For F_- and D_-, the moment directions are reversed (−− and −0+). In table 3 (non-zero field) we use the notation $F_{n\pm}$ to denote n ferromagnetic layers that are ferromagnetically coupled. + indicates that the moments are aligned parallel to the field and − that the moments are aligned antiparallel to the field. Disordered (paramagnetic) layers of

Ce-atoms with no net moment parallel to the field are denoted by 0.

Table 3. Average magnetic structures of CeSb in applied magnetic fields parallel to [001]. These structures consist of ferromagnetic (+ or -) and paramagnetic (0) layers of Ce^{3+} ions. N is the number of chemical cells contained in the magnetic cell along [001] (1 domain), and M is the period of the magnetic structure, i.e. the number of Ce^{3+} layers. σ/σ_F denotes the magnetization (σ) relative to the magnetization (σ_F) of a ferromagnetically ordered structure.

Temperature range (K)	L_o/N	N	M	σ/σ_F	Ce^{3+} layer sequence in M/2 chemical cells along [001]	Order (%)
CeSb T > 10	6/11	11	11	5/11	++00++00+00	45
	1/2	2	4	1/2	++00	50
	4/9	9	9	5/9	+++00++00	56
	2/5	5	5	3/5	+++00	60
	6/11	11	11	5/11	$\frac{1}{2}$ F_{11+} and $\frac{1}{2}$(++-++-++-)	
	1/2	2	4	1/2	$\frac{1}{2}$ F_{4+} and $\frac{1}{2}$(++--)	
	4/9	9	9	5/9	$\frac{1}{2}$ F_{9+} and $\frac{1}{2}$(+++-++-+--)	
	2/5	5	5	3/5	$\frac{1}{2}$ F_{5+} and $\frac{1}{2}$(+++--)	
CeSb T < 10	4/7	7	7	1/7	++--+-	100
	2/3	3	3	1/3	+-	100
	0	1	1	1	+	100
CeBi T < 25	1/2	2	4	1/2	+---	100

In order to determine the ordered magnetic moments accurately, and to test in detail the magnetic structures of CeSb, sets of nuclear and magnetic integrated intensities (from each type of domain) were measured on CeSb III at 4.4 K (phase VI), 14.1 K (phase III), 16.05 K (phase I) and in the paramagnetic phase at 77 K. To analyze these data a convenient description of the magnetic intensities is obtained by using Fourier components $\vec{E}(\vec{k})$ of the magnetic moment configuration $\{\vec{\mu}\}$ (cf. Lyons et al 1962, van Laar 1968). A detailed account of the Fourier representation of commensurable structures is given in Fischer et al 1977.

Each Fourier term corresponds to a pair of magnetic satellite peaks at $\vec{\tau}_{hk\ell} \pm \vec{k}_{00q_j}$ of the nuclear reflection at $\vec{\tau}_{hk\ell}$. The intensity of each satellite is proportional (for $q_j < 1$) to

$$I(\vec{k}_j) = 4A_\mu^2(\vec{k}_j)\{\tfrac{1}{2}r_o\gamma f(\vec{\kappa}_j)\}^2 \sin^2\delta, \quad A_\mu(\vec{k}_j) \equiv E(\vec{k}_j), \qquad (1)$$

where r_o is the classical electron radius, γ is the gyromagnetic ratio of the neutron, and $f(\vec{\kappa})$ is the neutron magnetic form

factor at the scattering vector $\vec{\kappa}$, and

$$\sin^2\delta = 1 - \frac{(\ell \pm q_j)^2}{h^2+k^2+(\ell \pm q_j)^2} .$$

For $q_j = 1$, $I(\vec{k}_j)$ should be multiplied by 4. In the case of an incommensurable q_j, $A_\mu(\vec{k}_j)$ is equal to μ, where μ is the maximum moment on any Ce^{3+} ion.

The observed and calculated intensities and the results of the refinements of the single crystal data at various fields and temperatures are listed for zero applied field in tables 4 to 7 and for non-zero field parallel to [001] in tables 8 to 12. The good agreement between the observed and calculated intensities is reflected in the low reliability factors (R or R_w) and implies

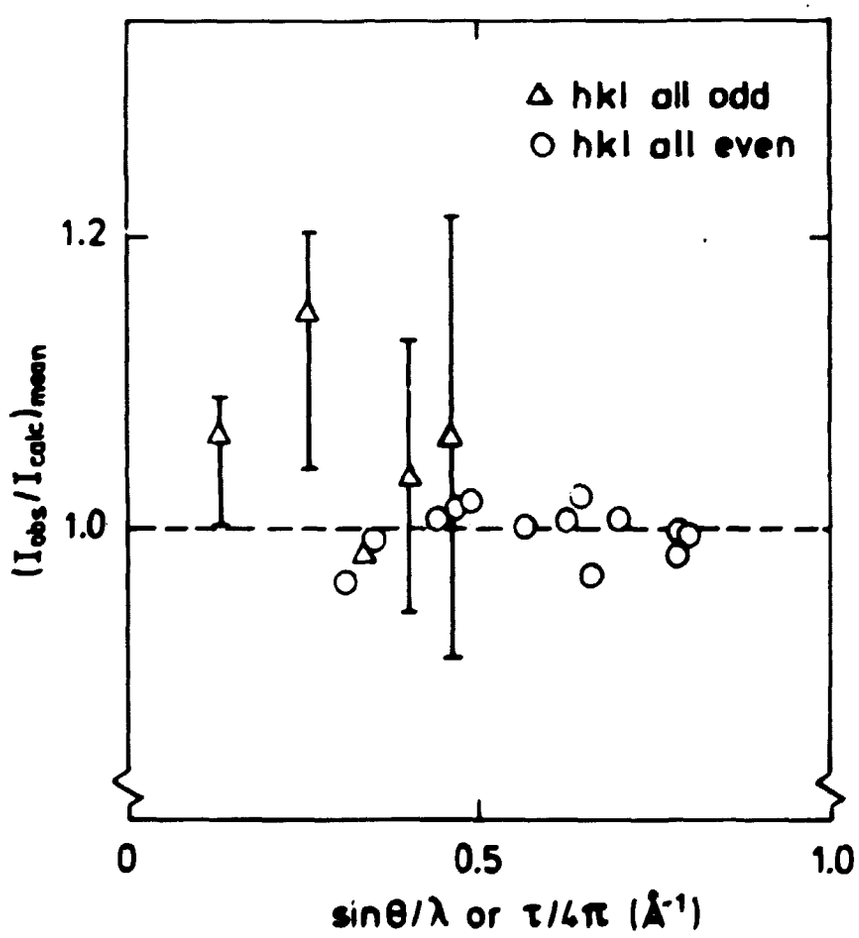

Figure 2. Average of I_{obs}/I_{calc} (table 4) over equivalent nuclear reflections versus scattering vector. The error bars indicate the upper and lower limits of I_{obs}/I_{calc}.

negligible extinction (when excluding intense reflections such as 200 and 022) and 1:1 stoichiometry of the sample. The R-factors given in tables 4 to 8 are defined as

$$R = \{\sum_j |I_{obs} - I_{calc}|_j\}/\sum_j (I_{obs})_j \text{ and}$$

$$R_w^2 = \{\sum_j [g_j (I_{obs} - I_{calc})_j]^2\}/\{\sum [gI_{obs}]_j^2\},\ g_j = \frac{1}{\Delta_j},$$

where Δ_j is the statistical uncertainty in $I_{obs,j}$. Usually, the inclusion of the anisotropy of the form factor f_J in the $M_J = J$ approximation resulted in slightly better agreement between the calculated and the observed intensities than the use of the form factor f_d in the dipolar approximation. Similarly, possible differences between the calculated and the true neutron magnetic form factor were allowed for by determining the Debye-Waller parameter of Ce from both the nuclear and the magnetic intensities. The goodness of the refinements is also illustrated in figures 2 and 3, which show the average over equivalent reflections of I_{obs}/I_{calc} versus scattering vector for the nuclear reflections (table 4) at 4.2 K (figure 2) and the magnetic satellites (tables 5 to 7) at 4.4, 14.1 and 16.05 K (figure 3).

For a powder sample, the intensity relation of equation (1) is modified to

$$I_m = 4C^2 \frac{(\frac{1}{2} r_o \gamma f(\vec{\kappa}) A_\mu(\vec{k}_j))^2 M}{\sin\theta \sin 2\theta} \times [1 - \frac{L^2}{H^2+K^2+L^2}] \times \exp[-2B_{Ce}(\sin\theta/\lambda)^2] \quad (2)$$

with tetragonal multiplicities M as well as H = h, K = k and L = $\ell \pm q$ referring to the f.c.c. unit cell. The Ce^{3+} neutron magnetic form factor $f(\vec{\kappa})$ was calculated in the dipolar approximation (Lander and Brun 1970).

From least-squares refinement of the integrated intensities of the nuclear peaks at 4.2 K, the scale factor C and the Debye-Waller parameter were obtained. The results are listed in table 13. The low R_n value indicates 1:1 stoichiometry of the powder sample investigated. In the refinement of the magnetic inten-

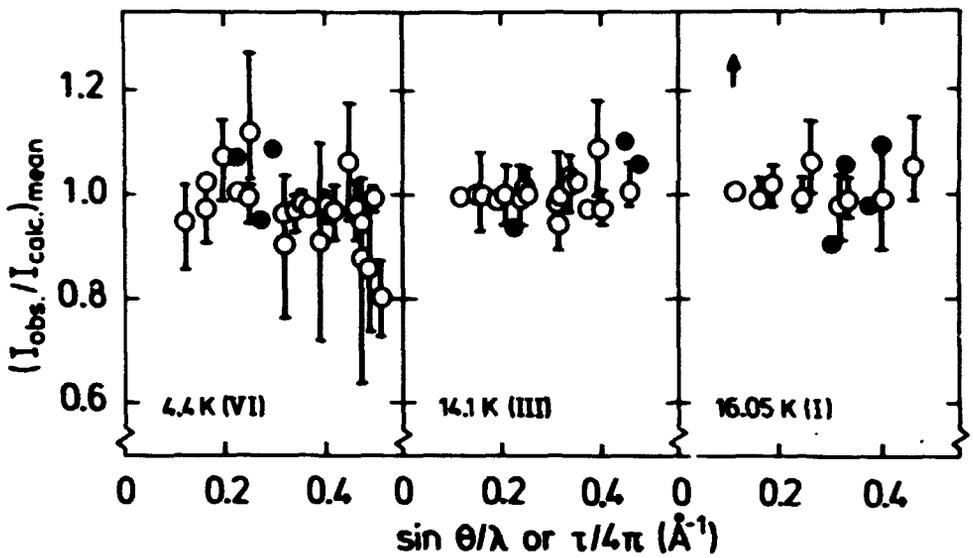

Figure 3. Average of I_{obs}/I_{calc} (tables 5 to 7) over equivalent magnetic satellites versus scattering vector. The error bars indicate the upper and lower limits of I_{obs}/I_{calc}. Filled signs indicate that only one reflection was measured.

sities the Debye-Waller parameter of Ce was also refined in order to allow for deviations of $f(\vec{\kappa})$ from the dipolar approximation. These results are also listed in table 13. The good agreement between the observed and the calculated magnetic intensities confirms the proposed model with moments along [001].

3. FOURIER REPRESENTATION OF THE MAGNETIC STRUCTURES OF CeSb

In real space, the Fourier representation of the magnetic moments of commensurable structures is

$$\vec{\mu}_n(\vec{r}_n) = \sum_{j=0}^{j=m} \vec{E}(\vec{k}_j)\cos(\vec{k}_j\vec{r}_n - \rho_j) \text{ with}$$

$$\rho_j = \arctan(\beta_j/\alpha_j) - \frac{2j}{M}\pi \ , \qquad (3)$$

where M is the number of layers of magnetic ions within a magnetic unit cell. In equation (3)

$$\vec{k}_j = \frac{2j\vec{\tau}}{M}_{001} \equiv q_j\tau_{001}\hat{e}_z$$

with $j = 0,1,\ldots,m$, where $2m = M-1$ for M odd, and $2m = M$ for M even. $\vec{E}(\vec{k}_j)$ is given by

$$\vec{E}(\vec{k}_j) = 2\hat{e}_z\sqrt{\alpha_j^2+\beta_j^2} \text{ and } \vec{E}(\vec{k}_{j'}) = \hat{e}_z\sqrt{\alpha_{j'}^2+\beta_{j'}^2} \text{ for } 2j' = 0 \text{ and } M \text{ (M even).}$$

$$\alpha_j = \frac{1}{M}\sum_{n=1}^{M} \mu_n(\vec{r}_n)\cos(\vec{k}_j\vec{r}_n + \frac{2j}{M}\pi) \text{ and}$$

$$\beta_j = \frac{1}{M}\sum_{n=1}^{M} \mu_n(\vec{r}_n)\sin(\vec{k}_j\vec{r}_n + \frac{2j}{M}\pi),$$

where n denotes the ferromagnetic layers of magnetic ions with moments parallel to [001] that are contained in the magnetic unit cell. For the f.c.c. Ce lattice, $\vec{r}_1 = \{0,0,0\}$; $\vec{r}_2 = \{1/2,0,1/2\}$, etc.

Below we give the Fourier representation of the magnetic structures observed in CeSb (cf. Fischer et al 1977 and Scheid 1968).

3.1. Zero Field Magnetic Structures

a) Phase I with moment sequence $D_- D_-$ corresponds to one $\vec{k}_j$ vector giving

$$\vec{\mu}_n = A_\mu(\tfrac{2}{3})\hat{e}_z \cos(\tfrac{2\vec{\tau}}{3}_{001}\vec{r}_n + \tfrac{5}{6}\pi) \text{ with } A_\mu(\tfrac{2}{3}) = \frac{2\mu}{\sqrt{3}} .$$

b) Phase II with moment sequence $F_+D_-D_-F_-D_+$ $F_+D_-D_-F_-D_+$ corresponds to six $\vec{k}_j$-vectors giving

$$\begin{aligned}\vec{\mu}_n = \hat{e}_z\{&A_\mu(\tfrac{2}{13})\cos(\tfrac{2\vec{\tau}}{13}_{001}\vec{r}_n - \tfrac{5}{26}\pi)\\ &+A_\mu(\tfrac{4}{13})\cos(\tfrac{4\vec{\tau}}{13}_{001}\vec{r}_n + \tfrac{3}{26}\pi)\\ &+A_\mu(\tfrac{6}{13})\cos(\tfrac{4\vec{\tau}}{13}_{001}\vec{r}_n - \tfrac{15}{26}\pi)\\ &+A_\mu(\tfrac{8}{13})\cos(\tfrac{8\vec{\tau}}{13}_{001}\vec{r}_n - \tfrac{7}{26}\pi)\\ &+A_\mu(\tfrac{10}{13})\cos(\tfrac{10\vec{\tau}}{13}_{001}\vec{r}_n - \tfrac{25}{26}\pi)\\ &+A_\mu(\tfrac{12}{13})\cos(\tfrac{12\vec{\tau}}{13}_{001}\vec{r}_n + \tfrac{9}{26}\pi)\},\end{aligned}$$

with $A_\mu(\tfrac{2}{13})/\mu \sim 0.2016$,

$A_\mu(\tfrac{4}{13})/\mu \sim 0.1692$,

$A_\mu(\tfrac{6}{13})/\mu \sim 0.1725$,

$A_\mu(\tfrac{8}{13})/\mu \sim 1.1934$,

$A_\mu(\tfrac{10}{13})/\mu \sim 0.1051$,

$A_\mu(\tfrac{12}{13})/\mu \sim 0.0648$,

c) Phase III with moment sequence $F_+D_-F_-$ $F_+D_-F_-$ corresponds to three k_j-vectors giving

$$\vec{\mu}_n = \hat{e}_z\{A_\mu(\tfrac{2}{7})\cos(\tfrac{2\vec{\tau}}{7}_{001}\vec{r}_n - \tfrac{5}{14}\pi)$$

$$+A_\mu(\tfrac{4}{7})\cos(\tfrac{4\vec{\tau}}{7}_{001}\vec{r}_n - \tfrac{3}{14}\pi)$$

$$+A_\mu(\tfrac{6}{7})\cos(\tfrac{6\vec{\tau}}{7}_{001}\vec{r}_n + \tfrac{13}{14}\pi)\},$$

with $A_\mu(\frac{2}{7})/\mu \sim 0.3583,$

$A_\mu(\frac{4}{7})/\mu \sim 1.2518,$ and

$A_\mu(\frac{6}{7})/\mu \sim 0.1376.$

d) Phase IV with moment sequence $F_+D_-F_-F_+$ $F_-D_+F_+F_-$ corresponds to four $\vec{k}_j$-vectors giving

$$\vec{\mu}_n = \hat{e}_z\{A_\mu(\tfrac{1}{9})\cos(\tfrac{1\vec{\tau}}{9}_{001}\vec{r}_n + \tfrac{1}{6}\pi)$$

$$+A_\mu(\tfrac{3}{9})\cos(\tfrac{3\vec{\tau}}{9}_{001}\vec{r}_n - \tfrac{1}{2}\pi)$$

$$+A_\mu(\tfrac{5}{9})\cos(\tfrac{5\vec{\tau}}{9}_{001}\vec{r}_n - \tfrac{1}{6}\pi)$$

$$+A_\mu(\tfrac{7}{9})\cos(\tfrac{7\vec{\tau}}{9}_{001}\vec{r}_n - \tfrac{5}{6}\pi)\},$$

with $A_\mu(\frac{1}{9})/\mu \sim 0.0809,$

$A_\mu(\frac{3}{9})/\mu \sim 0.3849,$

$A_\mu(\frac{5}{9})/\mu \sim 1.2603,$

$A_\mu(\frac{7}{9})/\mu \sim 0.1865$.

e) Phase V with moment sequence $F_+F_-F_+D_-F_-$ $F_+F_-F_+D_-F_-$ corresponds to five $\vec{k}_j$-vectors giving

$$\vec{\mu}_n = \hat{e}_z\{A_\mu(\tfrac{2}{11})\cos(\tfrac{2\vec{\tau}}{11}_{001}\vec{r}_n - \tfrac{17}{22}\pi)$$

$$+A_\mu(\tfrac{4}{11})\cos(\tfrac{4\vec{\tau}}{11}_{001}\vec{r}_n - \tfrac{1}{22}\pi)$$

$$+A_\mu(\tfrac{6}{11})\cos(\tfrac{6\vec{\tau}}{11}_{001}\vec{r}_n - \tfrac{7}{22}\pi)$$

$$+A_\mu(\tfrac{8}{11})\cos(\tfrac{8\vec{\tau}}{11}_{001}\vec{r}_n + \tfrac{9}{22}\pi)$$

$$+A_\mu(\tfrac{10}{11})\cos(\tfrac{10\vec{\tau}}{11}_{001}\vec{r}_n - \tfrac{19}{22}\pi)\},$$

with $A_\mu(\frac{2}{11})/\mu \sim 0.1169$,

$A_\mu(\frac{4}{11})/\mu \sim 0.3981$,

$A_\mu(\frac{6}{11})/\mu \sim 1.2646$,

$A_\mu(\frac{8}{11})/\mu \sim 0.2098$,

$A_\mu(\frac{10}{11})/\mu \sim 0.0534$.

f) Phase VI with moment sequence $F_+\ F_-$ corresponds to one $\vec{k}_j$-vector giving

$$\vec{\mu}_n = A_\mu(\tfrac{1}{2})\hat{e}_z\cos(\tfrac{1\vec{\tau}}{2}_{001}\vec{r}_n - \tfrac{\pi}{4}), \text{ with } A_\mu(\tfrac{1}{2}) = \sqrt{2}\mu\ .$$

3.2. Non-zero Field Magnetic Structures ($\vec{H}||[001]$).

a) The moment sequence ++00++00+00 corresponds to six $\vec{k}_j$-vectors giving

$$\vec{\mu}_n = \hat{e}_z\{A_\mu(0) + A_\mu(\tfrac{2}{11})\cos(\tfrac{2\vec{\tau}}{11}_{001}\vec{r}_n - \tfrac{5}{11}\pi)$$

$$+ A_\mu(\tfrac{4}{11})\cos(\tfrac{4\vec{\tau}}{11}_{001}\vec{r}_n + \tfrac{1}{11}\pi)$$

$$+ A_\mu(\tfrac{6}{11})\cos(\tfrac{6\vec{\tau}}{11}_{001}\vec{r}_n - \tfrac{4}{11}\pi)$$

$$+ A_\mu(\tfrac{8}{11})\cos(\tfrac{8\vec{\tau}}{11}_{001}\vec{r}_n + \tfrac{2}{11}\pi)$$

$$+ A_\mu(\tfrac{10}{11})\cos(\tfrac{10\vec{\tau}}{11}_{001}\vec{r}_n - \tfrac{15}{11}\pi)\},$$

with $A_\mu(0)/\mu \sim 0.9091,$

$A_\mu(\frac{2}{11})/\mu \sim 0.1081,$

$A_\mu(\frac{4}{11})/\mu \sim 0.2188,$

$A_\mu(\frac{6}{11})/\mu \sim 0.6388,$

$A_\mu(\frac{8}{11})/\mu \sim 0.1388,$

$A_\mu(\frac{10}{11})/\mu \sim 0.0948.$

b) The moment sequence ++00 corresponds to two $\vec{k}_j$-vector giving

$\vec{\mu}_n = \hat{e}_z\{A_\mu(0) + \cos(\frac{1}{2}\vec{\tau}_{001}\vec{r}_n - \frac{1}{4}\pi)\}$, with

$A_\mu(0) = \mu$ and $A_\mu(\frac{1}{2}) = \frac{\sqrt{2}}{2}\mu.$

c) The moment sequence +++00++00 corresponds to five $\vec{k}_j$-vectors giving

$$\vec{\mu}_n = \hat{e}_z\{A_\mu(0) + \cos(\tfrac{2}{9}\vec{\tau}_{001}\vec{r}_n - \tfrac{2}{9}\pi) + \cos(\tfrac{4}{9}\vec{\tau}_{001}\vec{r}_n - \tfrac{4}{9}\pi) + \cos(\tfrac{6}{9}\vec{\tau}_{001}\vec{r}_n + \tfrac{3}{9}\pi) + \cos(\tfrac{8}{9}\vec{\tau}_{001}\vec{r}_n + \tfrac{1}{9}\pi)\},$$

with $A_\mu(0)/\mu \sim 1.1111$

$A_\mu(\frac{2}{9})/\mu \sim 0.1450$

$A_\mu(\frac{4}{9})/\mu \sim 0.6399$

$A_\mu(\frac{6}{9})/\mu \sim 0.2222$

$A_\mu(\frac{8}{9})/\mu \sim 0.1182.$

d) The moment sequence +++00 corresponds to three $\vec{k}_j$-vectors giving

$$\vec{\mu}_n = \hat{e}_z\{A_\mu(0) + \cos(\tfrac{2}{5}\vec{\tau}_{001}\vec{r}_n - \tfrac{2}{5}\pi) + \cos(\tfrac{4}{5}\vec{\tau}_{001}\vec{r}_n + \tfrac{1}{5}\pi)\},$$

with $A_\mu(0)/\mu \sim 1.2000$

$A_\mu(\tfrac{2}{5})/\mu \sim 0.6472$

$A_\mu(\tfrac{4}{5})/\mu \sim 0.2472.$

e) The moment sequence ++--++-- corresponds to four $\vec{k}_j$-vectors giving

$$\vec{\mu}_n = \hat{e}_z\{A_\mu(0) + A_\mu(\tfrac{2}{7})\cos(\tfrac{2}{7}\vec{\tau}_{001}\vec{r}_n + \tfrac{2}{7}\pi) + A_\mu(\tfrac{4}{7})\cos(\tfrac{4}{7}\vec{\tau}_{001}\vec{r}_n - \tfrac{3}{7}\pi) + A_\mu(\tfrac{6}{7})\cos(\tfrac{6}{7}\vec{\tau}_{001}\vec{r}_n - \tfrac{1}{7}\pi)\},$$

with $A_\mu(0)/\mu \sim 0.2857$

$A_\mu(\tfrac{2}{7})/\mu \sim 0.4583$

$A_\mu(\tfrac{4}{7})/\mu \sim 1.2840$

$A_\mu(\tfrac{6}{7})/\mu \sim 0.3171.$

f) The moment sequence ++- corresponds to two $\vec{k}_j$-vector giving

$\vec{\mu}_n = \hat{e}_z\{A_\mu(0) + A_\mu(\tfrac{2}{3})\cos(\tfrac{2}{3}\vec{\tau}_{001}\vec{r}_n - \tfrac{1}{3}\pi)\}$, with

$A_\mu(0) = \tfrac{2}{3}\mu$ and $A_\mu(\tfrac{2}{3}) = \tfrac{4}{3}\mu.$

4. APPENDIX (Tables 4 to 13)

Table 4. Calculated (I_{calc}) and observed ($I_{obs}\pm\Delta$) integrated nuclear intensities at 4.4 K. Scattering lengths: b_{Ce} = 4.8 F and b_{Sb} = 5.6 F; Debye-Waller parameter B = 0.046(5) $Å^2$; scale factors C(λ) = 75.5(2) and C(λ/2) = 0.00366; lattice constant a = 6.400 Å and neutron wavelength λ = 1.033 Å. The intensity is proportional to $C(\lambda)^2\exp(-2B(\sin\theta/\lambda)^2)$. The agreement values are R_n = 1.5% and R_{nw} = 1.8%, where

$$R_n = \{\sum_j |I_{obs} - I_{calc}|_j\}/\sum_j (I_{obs})_j \text{ and}$$

$$R^2_{nw} = \{\sum_j [g_j(I_{obs}-I_{calc})_j]^2\}/\{\sum_j [gI_{obs}]^2_j\},\ g_j = 1/\Delta_j.$$

h	k	ℓ	I_{obs}	±Δ	I_{calc}	h	k	ℓ	I_{obs}	±Δ	I_{calc}
1	1	1	2823	1595	2591	8	0	0	97079	597	96558
-1	1	1	2787	1596	2591	-8	0	0	99229	603	96558
-1	-1	1	2599	1597	2591	0	8	0	96659	597	96558
1	-1	1	2818	1598	2591	0	-8	0	96612	599	96558
3	1	1	1233	723	1184	8	2	0	97712	596	95628
-3	1	1	1416	724	1184	-8	2	0	98020	598	95628
1	3	1	1375	723	1184	-8	-2	0	97382	598	95628
-1	3	1	1424	723	1184	8	-2	0	97152	594	95628
4	0	0	154032	852	160016	2	8	0	96812	596	95628
-4	0	0	153697	854	160016	-2	8	0	97875	598	95628
0	4	0	153827	854	160016	-2	-8	0	98765	601	95628
0	-4	0	155075	855	160016	2	-8	0	97720	598	95628
3	3	1	890	546	905	6	6	0	91534	581	94976
4	2	0	142449	795	144929	-6	6	0	91856	581	94976
-4	2	0	143082	797	144929	-6	-6	0	93089	586	94976
-4	-2	0	144037	799	144929	6	-6	0	91679	581	94976
4	-2	0	143852	799	144929	8	4	0	95447	589	94459
2	4	0	143559	795	144929	-8	4	0	95644	591	94459
-2	4	0	143769	797	144929	-8	-4	0	96157	591	94459
-2	-4	0	143769	799	144929	8	-4	0	94289	587	94459
2	-4	0	145779	803	144929	4	8	0	94597	587	94459
5	1	1	729	462	773	-4	8	0	94874	587	94459
1	5	1	873	463	773	-4	-8	0	95442	593	94459
4	4	0	120121	697	119302	4	-8	0	95244	589	94459
-4	4	0	121803	699	119302	8	6	0	96273	596	97936
-4	-4	0	119236	695	119302	-8	6	0	96696	598	97936
4	-4	0	119786	695	119302	-8	-6	0	97171	600	97936
5	3	1	633	410	695	8	-6	0	97536	598	97936
3	5	1	844	414	695	6	8	0	96031	594	97936
6	0	0	116484	676	114124	-6	8	0	97111	600	97936
-6	0	0	116794	676	114124	-6	-8	0	98368	600	97936
0	6	0	114189	672	114124	6	-8	0	96776	598	97936
0	-6	0	115609	676	114124	10	0	0	96861	596	97936
6	2	0	111658	658	109914	-10	0	0	97773	600	97936
-6	2	0	112816	660	109914	0	10	0	94993	592	97936
-6	-2	0	112391	660	109914	0	-10	0	95133	598	97936
6	-2	0	111876	658	109914	10	2	0	100613	608	99619
2	6	0	111183	658	109914	-10	2	0	99393	606	99619
-2	6	0	112261	660	109914	-10	-2	0	101490	610	99619
-2	-6	0	112731	660	109914	10	-2	0	99573	606	99619
2	-6	0	113203	662	109914	2	10	0	99073	606	99619
6	4	0	102440	619	101263	-2	10	0	98155	604	99619
-6	4	0	101912	619	101263	-2	-10	0	99100	606	99619
-6	-4	0	102060	619	101263	2	-10	0	98238	606	99619
6	-4	0	100320	615	101263						
4	6	0	100427	615	101263						
-4	6	0	101855	621	101263						
-4	-6	0	102060	621	101263						
4	-6	0	101647	617	101263						

Table 5. Integrated magnetic intensities of CeSb III at 4.4 K. The neutron magnetic form factor f_J is calculated in the $M_J = J$ approximation (Lander and Brun 1970). f_d is the form factor in the dipolar approximation. The total moment $\mu = 2.06(4^\circ)\ \mu_B$ and amplitude $A_\mu = 2.91(7^\circ)\ \mu_B$.

X-domains

$A_\mu^X = 1.62(1)\ \mu_B$, $B_{Ce} = 0.1(2)\ A^2$

for $f = f_J$

$R_m = 6.1\%$, $R_{mw} = 6.6\%$

for $f = f_d$

$R_m = 9.2\%$, $R_{mw} = 9.2\%$

h	k	ℓ	I_{obs}	±Δ	I_{calc}
0.504	0	0	0	134	0
1.496	0	0	0	134	0
0.504	2	0	10914	67	10757
-0.504	2	0	11032	69	10757
-0.504	-2	0	10859	134	10757
0.504	-2	0	11028	137	10757
1.496	2	0	6169	55	5637
-1.496	2	0	6173	105	5637
-1.496	-2	0	6035	103	5637
1.496	-2	0	5978	104	5637
2.504	0	0	0	92	0
2.504	2	0	2624	80	2435
-2.504	2	0	2514	80	2435
-2.504	-2	0	2708	79	2435
2.504	-2	0	2799	87	2435
3.496	0	0	0	34	0
3.496	2	0	1158	34	1109
0.504	4	0	3341	85	3424
-0.504	4	0	3240	88	3424
1.496	4	0	2794	42	2771
4.504	0	0	0	39	0
2.504	4	0	1856	37	1929
4.504	2	0	580	30	528
3.496	4	0	1269	36	1247
5.496	0	0	0	30	0
5.496	2	0	195	23	267
0.504	6	0	855	62	1129
-0.504	6	0	721	56	1129
4.504	4	0	760	31	758
1.496	6	0	1000	70	1023
2.504	6	0	742	62	847
6.504	0	0	0	62	0
6.504	2	0	0	31	145
0.496	1	1	17848	162	20041
-0.496	1	1	18453	164	20041
1.504	1	1	6504	112	6476
-1.504	1	1	6429	115	6476
2.496	1	1	2120	75	1978
3.504	1	1	825	61	757

Y-domains

$A_\mu^Y = 1.21(1)\ \mu_B$, $B_{Ce} = -0.2(3)\ A^2$

for $f = f_J$

$R_m = 8.2\%$, $R_{mw} = 8.1\%$

for $f = f_d$

$R_m = 10.4\%$, $R_{mw} = 10.1\%$

h	k	ℓ	I_{obs}	±Δ	I_{calc}
0	0.504	0	0	85	0
0	1.496	0	0	85	0
2	0.504	0	6392	40	6089
2	-0.504	0	6273	57	6089
-2	0.504	0	6290	109	6089
-2	-0.504	0	6247	111	6089
2	1.496	0	3524	52	3213
-2	1.496	0	3380	84	3213
-2	-1.496	0	3674	107	3213
2	-1.496	0	3618	92	3213
0	2.504	0	0	92	0
2	2.504	0	1453	52	1407
-2	2.504	0	1710	74	1407
-2	-2.504	0	1476	73	1407
2	-2.504	0	1786	81	1407
2	3.496	0	655	59	854
4	0.504	0	1874	74	2021
4	-0.504	0	1976	73	2021
4	1.496	0	1535	72	1647
4	2.504	0	1149	68	1163
2	4.504	0	231	65	321
4	3.496	0	704	61	768
2	5.496	0	0	61	168
6	0.504	0	511	56	715
6	-0.504	0	735	65	715
4	4.504	0	428	69	480
6	1.496	0	481	76	652
6	2.504	0	402	71	548
2	6.504	0	0	71	95
1	0.496	1	10365	137	11284
-1	0.496	1	9685	132	11264
1	1.504	1	3501	87	3665
-1	1.504	1	3698	91	3665
3	0.496	1	3100	87	3276
3	1.504	1	2303	80	2422

Z-domains

$A_\mu^Z = 2.09(1)\ \mu_B$, $B_{Ce} = 0.4(1)\ A^2$

for $f = f_J$

$R_m = 2.1\%$, $R_{mw} = 2.8\%$

for $f = f_d$

$R_m = 2.6\%$, $R_{mw} = 2.9\%$

h	k	ℓ	I_{obs}	±Δ	I_{calc}
1	1	0.496	25986	175	26137
-1	1	0.496	26108	176	26137
-1	-1	0.496	25877	177	26137
1	-1	0.496	26588	179	26137
3	1	0.496	8899	113	8791
1	3	0.496	9021	113	8791
3	3	0.496	4934	91	4737
5	1	0.496	2951	81	2916
1	5	0.496	2777	83	2916
5	3	0.496	1711	71	1859
3	5	0.496	1923	73	1859
2	0	0.504	18492	152	18319
0	2	0.504	18445	149	18319
-2	0	0.504	19081	160	18319
0	-2	0.504	18744	165	18319
2	2	0.504	10859	86	10685
-2	2	0.504	10828	121	10685
-2	-2	0.504	10629	119	10685
4	0	0.504	5352	95	5482
0	4	0.504	5252	91	5482
4	2	0.504	3984	87	4123
2	4	0.504	4168	87	4123
4	4	0.504	2068	75	2063
6	0	0.504	1989	83	1687
0	6	0.504	1607	71	1687
6	2	0.504	1361	67	1395
2	6	0.504	1411	68	1395
2	0	1.496	11754	131	11679
0	2	1.496	11602	130	11679
1	1	1.504	13137	138	13810
-1	1	1.504	12563	137	13810

*Includes the uncertainty in the scale factor C arising from an uncertainty in the nuclear scattering lengths of $\Delta b = \pm 0.1$ F.

Table 6. Integrated magnetic intensities of CeSb III at 14.1 K. A scale factor C = 77.1(3) yields $A_\mu(4/7)$ = 2.54(5) μ_B, $A_\mu(2/7)$ = 0.7(1) μ_B, and μ = 2.03 μ_B.

X-domains

$A_\mu^X(4/7)$ = 1.49(1) μ_B, B_{Ce} = 0.4(1) Å^2

for $f = f_J$

R_m = 1.3%, R_{mw} = 1.6%

for $f = f_d$

R_m = 3.3%, R_{mw} = 4.5%

$A_\mu^X(2/7)$ = 0.29(2) μ_B, B_{Ce} = 0(2) Å^2

for $f = f_J$

R_m = 6.8%, R_{mw} = 6.9%

for $f = f_d$

R_m = 6.9%, R_{mw} = 7.0%

h	k	ℓ	I_{obs}	±Δ	I_{calc}
1.428	0	0	0	40	0
0.572	2	0	9007	109	9137
-0.572	2	0	9168	113	9137
1.428	2	0	5253	88	5176
2.572	2	0	2072	61	1969
3.428	2	0	943	49	982
0.572	4	0	2877	73	2845
-0.572	4	0	2824	71	2845
1.428	4	0	2347	68	2354
2.572	4	0	1507	58	1538
4.572	2	0	410	42	410
1.713	0	0	0	12	0
0.287	2	0	411	19	381
-0.287	2	0	356	18	381
1.713	2	0	143	15	152
2.287	2	0	97	13	92

Y-domains

$A_\mu^Y(4/7)$ = 1.08(1) μ_B, B_{Ce} = 0.5(2) Å^2

for $f = f_J$

R_m = 3.1%, R_{mw} = 3.6%

for $f = f_d$

R_m = 3.7%, R_{mw} = 4.6%

$A_\mu^Y(2/7)$ = 0.20(2) μ_B, B_{Ce} = 1(3) Å^2

for $f = f_J$

R_m = 5.3%, R_{mw} = 5.3%

for $f = f_d$

R_m = 5.1%, R_{mw} = 4.9%

h	k	ℓ	I_{obs}	±Δ	I_{calc}
2	0.572	0	4739	92	4751
2	-0.572	0	4848	89	4751
2	1.428	0	2598	71	2688
2	2.572	0	999	50	1019
2	3.428	0	471	45	507
4	0.572	0	1366	56	1466
4	-0.572	0	1554	57	1466
4	1.428	0	1291	57	1212
4	2.572	0	765	49	789
2	4.572	0	248	49	210
2	0.287	0	169	16	179
2	-0.287	0	187	15	179
2	1.713	0	75	18	71
2	2.287	0	40	17	43

Z-domains

$A_\mu^Z(4/7)$ = 1.75(1) μ_B, B_{Ce} = 0.2(1) Å

for $f = f_J$

R_m = 1.3%, R_{mw} = 1.9%

for $f = f_d$

R_m = 1.2%, R_{mw} = 1.8%

$A_\mu^Z(2/7)$ = 0.56(1) μ_B, B_{Ce} = 0.4(2) Å

for $f = f_J$

R_m = 3.7%, R_{mw} = 4.2%

for $f = f_d$

R_m = 4.5%, R_{mw} = 4.9%

h	k	ℓ	I_{obs}	±Δ	I_{calc}
1	1	0.428	19661	147	19749
-1	1	0.428	19783	147	19749
3	1	0.428	6687	91	6616
-3	1	0.428	6729	92	6616
1	3	0.428	6642	98	6616
-1	3	0.428	6582	90	6616
3	3	0.428	3561	72	3615
-3	3	0.428	3890	79	3615
5	1	0.428	2128	61	2259
-5	1	0.428	2201	63	2259
1	5	0.428	2304	63	2259
-1	5	0.428	2179	62	2259
5	3	0.428	1449	55	1463
-5	3	0.428	1550	57	1463
3	5	0.428	1445	58	1463
-3	5	0.428	1436	55	1463
2	0	0.287	1463	25	1449
0	2	0.287	1470	24	1449
2	2	0.287	775	20	826
4	0	0.287	375	17	419
0	4	0.287	453	18	419
4	2	0.287	326	17	314
2	4	0.287	318	16	314
4	4	0.287	172	20	156
6	0	0.287	135	17	127

Table 7. Integrated magnetic intensities of CeRh III at 16.05 K. A scale factor C = 77.2(3) yields A_b = 1.94(5) μ_B and μ = 1.68(6) μ_B.

X-domain	Y-domain	Z-domain
A_b^X = 1.17(2) μ_B, R_{Cr} = 0.3(4) Å^2	A_b^Y = 0.95(2) μ_B, R_{Cr} = 0.6(3) Å^2	A_b^Z = 1.22(1) μ_B, R_{Cr} = 0.4(1) Å^2
for $f = f_3$	for $f = f_3$	for $f = f_3$
R_b = 3.20, R_{Rh} = 6.70	R_b = 6.00, R_{Rh} = 6.50	R_b = 2.20, R_{Rh} = 2.00
for $f = f_6$	for $f = f_6$	for $f = f_6$
R_b = 6.50, R_{Rh} = 5.60	R_b = 6.70, R_{Rh} = 5.00	R_b = 2.10, R_{Rh} = 2.00

h	k	ℓ	I_{obs}	±Δ	I_{calc}	h	k	ℓ	I_{obs}	±Δ	I_{calc}	h	k	ℓ	I_{obs}	±Δ	I_{calc}
1.333	0	0	136	36	0	2	0.667	0	3057	71	3522	1	1	0.333	9954	116	9089
0.667	2	0	5388	84	5436	2	-0.667	0	3528	78	3522	-1	1	0.333	9885	113	9089
-0.667	2	0	5388	84	5436	2	1.333	0	2206	58	2252	3	1	0.333	3137	69	3160
1.333	2	0	3679	73	3682	2	2.667	0	836	53	732	-3	1	0.333	3200	70	3160
2.667	2	0	1115	51	1130	4	0.667	0	1186	51	1126	1	3	0.333	3089	70	3160
3.333	2	0	804	42	666	4	-0.667	0	1000	50	1126	-1	3	0.333	3076	70	3160
-0.667	4	0	1776	61	1762	4	1.333	0	2020	60	971	3	3	0.333	1739	57	1686
4.667	2	0	265	30	262	4	2.667	0	570	57	591	-3	3	0.333	1611	56	1686
												5	1	0.333	1141	50	1020
												-5	1	0.333	1020	52	1020
												1	5	0.333	1006	52	1020
												-1	5	0.333	915	50	1020
												5	3	0.333	751	54	652
												-5	3	0.333	645	57	652
												3	5	0.333	683	48	652
												-3	5	0.333	670	60	652
												2	0	0.667	6852	140	6101

Table 8. The observed, corrected, integrated intensities of CeRh III at 4.2 K for increasing and decreasing magnetic fields $\vec{H}$ applied parallel to [0$\bar{1}$1]. The standard deviations are given in parentheses. μ_1 and μ_2 are the ordered moments derived from the most intense satellites (q = 0) and from 111, respectively. $\mu = \frac{1}{2}(\mu_1 + \mu_2)$. For H = 1.5 T and μ = 1.8 μ_B we calculate $I_{calc}(1/7) \sim 2I_{obs}(2/7)$.

H (T)	q (r.l.u.)	Observed intensities I_{obs} 02q	q20	2q0	μ_1 (μ_B)	q (r.l.u.)	I_{obs} 111	μ_2 (μ_B)	μ (μ_B)
0	1/2	32221(122)	6654(70)	5905(68)	2.06	0	3291(34)	0	2.1
0.52	1/2	30579(109)	7995(65)	8466(68)	2.02	0	3312(40)	0	2.0
1.06	1/2	26836(110)	7832(64)	8171(66)	2.02	0	3239(39)	0	2.0
	1/2		770(31)	336(26)	0.32				
1.50	6/7	37195(128)			2.10	0	4037(42)	1.54	1.8
	2/7	2782(40)							
2.19	2/3	40744(136)	0	0	2.15	0	10304(62)	2.01	2.1
2.50	2/3	40652(117)	0	0	2.14	0	10790(62)	2.07	2.1
3.00	2/3	40701(74)	0	0	2.15	0	11040(61)	2.10	2.1
3.50	2/3	41085(104)	0	0	2.16	0	11034(85)	2.10	2.1
4.00					-	0	68898(206)	2.04	2.0
4.22					-	0	67769(102)	2.02	2.0
2.90	2/3	41267(105)	0	0	2.10	0	11065(87)	2.16	2.2
2.05	2/3	41304(105)	0	0	2.16	0	11114(86)	2.10	2.1
1.40	6/7	38219(102)	0	0	2.13	0	4647(50)	2.03	2.1
0	1/2	31932(169)	9062(97)	5319(78)	2.10	0	3305(51)	0	2.1

Table 9. The observed, corrected, integrated intensities of CeSb III at 10.9 K for increasing and decreasing magnetic fields applied parallel to [001] (cf. table 3). Using the values of μ determined from the experiment, we find $I_{calc}(4/11) \sim 0.6 I_{obs}(4/11)$ for H < 1.5 T and $I_{calc}(4/5) \sim 2 I_{obs}(4/5)$ for 3.5 T < H < 4.5 T.

H (T)	q (r.l.u.)	Observed intensities I_{obs} 02q	q20	2q0	μ_1 (μ_B)	q (r.l.u.)	I_{obs} 111	μ_2 (μ_B)	μ (μ_B)
0	4/11	4518(62)							
	6/11	20780(98)	5643(64)	8214(72)	2.07	0	2670(46)	0	2.1
0.52	4/11	5309(66)							
	6/11	21136(98)	5668(63)	8081(70)	2.08	0	2775(48)	0	2.1
1.00	4/11	4494(62)							
	6/11	20018(97)	5076(71)	8040(68)	2.02	0	2766(46)	0	2.0
1.50	4/11	4278(61)							
	6/11	17680(92)	5784(63)	9288(74)	2.01	0	2777(47)	0	2.0
2.25	2/3	38427(124)	0	0	2.11	0	9357(64)	1.98	2.1
2.50	2/3	38185(125)	0	0	2.10	0	9178(64)	1.95	2.0
2.75	4/9	10277(75)	0	0	2.21	0	20770(82)	1.96	2.1
3.00	4/9	10083(104)	0	0	2.18	0	20370(116)	1.93	2.1
3.50	2/5	9813(73)	0	0	2.11				
	4/5	725(54)				0	22862(122)	1.92	2.0
4.00	2/5	9771(101)	0	0	2.11				
	4/5	614(54)				0	23465(128)	2.03	2.1
4.50	2/5	8838(100)	0	0	2.00				
	4/5	617(48)				0	24879(125)	2.00	2.0
5.00						0	54808(173)	1.84	1.8
3.90	2/5	10125(104)	0	0	2.14				
	4/5	721(53)				0	23471(125)	1.93	2.0
2.90	4/9	9955(105)	0	0	2.16	0	20271(80)	1.93	2.1
2.50	2/3	30257(110)	0	0	1.87	0	7808(78)	1.74	1.8
1.00	4/11	794(73)							
	6/11	5619(96)	5356(83)	18362(126)	1.91	0	2929(75)	0	1.9
0	6/11	6258(91)	5218(84)	17291(124)	1.89	0	2421(69)	0	1.9

Table 10. The observed, corrected, integrated intensities of CeSb III at 16.1 K for increasing and decreasing magnetic fields applied parallel to [001] (cf. table 3). Using the values of μ determined from the experiment, we find $I_{calc}(4/11) \sim 0.4 I_{obs}(4/11)$ and $I_{calc}(8/11) \sim 0.2 I_{obs}(8/11)$ for H < 1.5 T (H increasing), $I_{calc}(6/9) \sim 0.8 I_{obs}(6/9)$ for H = 4.79 T and $I_{calc}(q) \sim I_{obs}(q)$ for q = 2/11, 4/11 and 8/11 for H = 1.4 T (H decreasing).

H (T)	q (r.l.u.)	Observed intensities I_{obs} 02q	q20	2q0	μ_1 (μ_B)	q (r.l.u.)	I_{obs} 111	μ_2 (μ_B)	μ (μ_B)
0	2/3	6133(94)	2170(72)	3440(79)	1.27	0	2432(61)	0	1.3
1.00	4/11	2382(78)							
	6/11	7613(102)	0	0	1.81	0	7863(84)	1.28	1.6
	8/11	1597(80)							
1.50	4/11	2716(71)							
	6/11	7708(69)	0	0	1.82	0	9126(89)	1.36	1.6
2.00	1/2	9112(103)	0	0	1.77	0	11342(88)	1.44	1.6
2.50	1/2	8773(99)	0	0	1.74	0	12127(94)	1.50	1.6
3.00	1/2	9255(100)	0	0	1.79	0	13985(100)	1.64	1.7
3.50	1/2	9030(99)	0	0	1.77	0	14997(102)	1.70	1.7
3.75	1/2	8686(96)	0	0	1.73	0	15340(100)	1.72	1.7
4.50	4/9	7355(93)	0	0	1.75	0	17135(104)	1.66	1.7
4.79	4/9	7452(88)	0	0	1.76				
	6/9	1176(83)				0	18225(107)	1.71	1.7
4.00	1/2	8707(147)	0	0	1.73	0	16172(164)	1.78	1.8
3.00	1/2	11425(166)	0	0	1.99	0	14010(151)	1.63	1.8
2.00	1/2	11789(168)	0	0	2.02	0	12362(144)	1.51	1.8
1.40	2/11	277(59)							
	4/11	1155(73)							
	6/11	7979(149)	0	0	1.85	0	9852(130)	1.44	1.7
	8/11	218(52)							
0.80	6/11	9559(155)	0	0	2.02	0	9211(127)	1.37	1.7
0	2/3	9123(150)	2652(97)	4154(113)	1.48	0	2505(74)	0	1.5

Table 11. The observed (I_{obs}) and calculated (I_{calc}) magnetic intensities in CeSb III at 4.2 K and at H = 2.50 T applied parallel to [001]. From the satellite intensities, we find μ_1 = 1.9(2) μ_B with R = 9.6% and R_{sw} = 11.5%. From the ferromagnetic intensities, we find μ_2 = 1.8(2) μ_B with R_f = 13.0% and R_{fw} = 14.5%.

Satellite intensities				
h	k	ℓ	I_{obs}	I_{calc}
1	1	0.333	2001(5)	1877
1	3	0.333	665(3)	605
3	3	0.333	336(3)	324
1	5	0.333	195(2)	199
5	1	0.333	208(2)	199
2	0	0.667	960(3)	1177
0	2	0.667	1259(4)	1177
2	2	0.667	788(4)	704
0	4	0.667	376(2)	366
2	4	0.667	285(2)	277
4	2	0.667	225(2)	277
4	4	0.667	165(2)	139
2	6	0.667	87(2)	95
4	6	0.667	62(2)	56

Ferromagnetic intensities				
h	k	ℓ	I_{obs}	I_{calc}
1	1	1	330(4)	296
-1	1	1	343(4)	296
-1	-1	1	240(4)	296
1	-1	1	287(4)	296
1	3	1	137(4)	132
3	1	1	94(4)	172
3	3	1	95(3)	79
1	5	1	53(4)	54

Table 12. The observed (I_{obs}) and calculated (I_{calc}) magnetic intensities in CeSb III at 4.2 K and at H = 4.02 T applied parallel to [001]. From these intensities we find μ_2 = 1.8(2) μ_B with R_f = 10.8% and R_{fw} = 12.6%.

Ferromagnetic intensities				
h	k	ℓ	I_{obs}	I_{calc}
1	1	1	2819(6)	2546
-1	1	1	2846(6)	2546
-1	-1	1	2076(5)	2546
1	-1	1	2521(6)	2546
3	1	1	1185(5)	1109
1	3	1	1248(5)	1109
-1	3	1	1218(5)	1109
-3	1	1	867(5)	1109
3	3	1	716(4)	654
1	5	1	421(4)	435
-1	5	1	412(4)	435
5	5	1	124(3)	164

Table 13. The observed and calculated integrated nuclear and magnetic intensities of CeSb powder at 4.2 K. The scale factor C = 13.9(1).

Nuclear intensities

B = 0.4(1) $Å^2$

R_n = 2.0%, R_{nw} = 1.9%

h	k	ℓ	I_{obs}	±Δ	I_{calc}
1	1	1	756	116	822
2	0	0	80484	338	79288
2	2	0	83482	364	84550
3	1	1	0	212	772
2	2	2	39882	284	40753
4	0	0	24613	256	25502
3	3	1	0	226	565
4	2	0	95851	396	94757

Magnetic intensities

B_{Ce} = 0.8(3) $Å^2$

A_μ(6/11) = 2.74(6) μ_B, μ = 2.17(5) μ_B

for $f = f_d$

R_m = 5.7%, R_{mw} = 4.8%

h	k	ℓ	I_{obs}	±Δ	I_{calc}	
0	0	0.55	0	270	0	
0	0	1.45	18984	292	0	18919
1	1	0.45			18919	
2	0	0.55	12828	335	9131	13674
1	1	1.55			4343	
2	0	1.45	4594	211	4255	
0	0	2.55	0	211	0	
1	1	2.45	5034	455	1161	5433
2	2	0.55			4272	
2	2	1.45	11169	241	2739	10689
3	1	0.45			6697	
2	0	2.55			1253	
0	0	3.45	0	355	0	
3	1	1.55	3641	355	4274	
2	2	2.55	1782	197	1195	1489
1	1	3.55			294	
2	0	3.45	4276	307	485	4712
3	1	2.45			2392	
4	0	0.55			1835	
4	0	1.45	2795	196	1459	3081
3	3	0.45			1622	
2	2	3.45	5179	499	599	4761
4	2	0.55			2879	
3	3	1.55			1283	
0	0	4.55	0	499	0	

5. REFERENCES

COOPER, B.R. (1976a). Lattice effects and the magnetic behaviour of rare earth compounds. In: Magnetism in Metals and Metallic Compounds. Edited by J.T. Lopuszanski, A. Pekalski, and J. Przystawa (Plenum, New York) 225-263.

COOPER, B.R. (1976b). Anisotropic behaviour and complex colinear magnetic structures of cerium and actinide intermetallics. To appear in the Proceedings of the 2nd International Conference on the Electronic Structure of the Actinides, Wroclaw, Poland, September 1976.

FISCHER, P., LEBECH, B., MEIER, G., RAINFORD, B.D., and VOGT, O. (1977). Magnetic phase transitions of CeSb:I Zero applied magnetic field. J. Phys. C. Solid State Phys. (in print).

LANDER, G.H. and BRUN, T.O. (1970). Calculation of neutron magnetic form factors for rare-earth ions. J. Chem. Phys. 53, 1387-1391.

LEBECH, B. and NIELSEN, M. (1975). Intensity and resolution of a general scan in reciprocal space. In: New Methods and Techniques in Neutron Diffraction. Proceedings of the Neutron Diffraction Conference. Petten, August 5-6, 1975 (Reactor Centrum Netherland) (RCN-234) 466-486.

LYONS, D.H., KAPLAN, T.A., DWIGHT, K., and MENYUK, N. (1962). Classical theory of the ground spin-state in cubic spinels. Phys. Rev. 126, 540-555.

MEIER, G., FISCHER, P., HÄLG, W., LEBECH, B., RAINFORD, B.D., and VOGT, O. (1978). Magnetic phase transitions of CeSb:II Effects of applied magnetic fields. Accepted for publication in J. Phys. C. Solid State Phys.

NERESON, N. and STRUEBING, V. (1972). Neutron diffraction studies of DySb, NdSb, and CeSb. AIP Conference Proceedings 5, 1385-1389.

SCHEID, F.J. (1968. Schaum's outline of theory and problems of numerical analysis. Chapter 24 (McGraw-Hill, New York).

VAN LAAR, B. (1968). Determination of magnetic structure. RCN-92, 145 pp.

ISBN 87-550-0503-9